Title:

A single-dose MCMV-based vaccine elicits long-lasting immune protection in mice against distinct SARS-CoV-2 variants

Authors:

Kristin Metzdorf[1, ‡], Henning Jacobsen[1, ‡], Yeonsu Kim[1, ‡], Luiz Gustavo Teixeira Alves[2], Upasana Kulkarni[1], Kathrin Eschke[1], M. Zeeshan Chaudhry[1], Markus Hoffmann[4, 5], Federico Bertoglio[6], Maximilian Ruschig[6], Michael Hust[6], Maja Cokarić Brdovčak[7], Jelena Materljan[7, 8], Marko Šustić[7], Astrid Krmpotić[8], Stipan Jonjić[7], Marek Widera[9], Sandra Ciesek[9, 10, 11], Stefan Pöhlmann[4, 5], Markus Landthaler[2, 3], Luka Čičin-Šain[1, 12, *]

Affiliations:

[1]   Department of Viral Immunology, Helmholtz Centre for Infection Research, Braunschweig, Germany

[2]   Berlin Institute for Medical Systems Biology (BIMSB), Max Delbrück Center for Molecular Medicine in the Helmholtz Association (MDC), Berlin, Germany

[3]   Institute for Biology, Humboldt-Universität zu Berlin, Berlin, Germany

[4]   Infection Biology Unit, German Primate Center – Leibniz Institute for Primate Research, Göttingen, Germany

[5]   Faculty of Biology and Psychology, Georg-August-University Göttingen, Göttingen, Germany

[6]   Department of Medical Biotechnology, Institute for Biochemistry, Biotechnology and Bioinformatics, Technische Universität Braunschweig, Braunschweig, Germany

[7]   Center for Proteomics, University of Rijeka, Faculty of Medicine, Rijeka, Croatia

[8]   Department of Histology and Embryology, University of Rijeka, Faculty of Medicine, Rijeka, Croatia

[9]   Institute for Medical Virology, University Hospital Frankfurt, Goethe University Frankfurt, Frankfurt am Main, Germany

[10]   Fraunhofer Institute for Translational Medicine and Pharmacology ITMP, Frankfurt am Main, Germany

[11]   German Centre for Infection Research (DZIF), External partner site Frankfurt, Germany

[12]   Centre for Individualized Infection Medicine (CiiM), a joint venture of HZI and MHH, Hannover, Germany

‡   These authors contributed equally

*   Correspondence: luka.cicin-sain@helmholtz-hzi.de

Abstract:

Current vaccines against COVID-19 elicit immune responses that are overall strong but wane rapidly. As a consequence, the necessary booster shots have led to vaccine fatigue. Hence, vaccines that would provide lasting protection against COVID-19 are needed, but are still unavailable. Cytomegaloviruses (CMV) elicit lasting and uniquely strong immune responses. Used as vaccine vectors, they may be attractive tools that obviate the need for boosters. Therefore, we tested the murine CMV (MCMV) as a vaccine vector against COVID-19 in relevant preclinical models of immunization and challenge. We have previously developed a recombinant murine CMV (MCMV) vaccine vector expressing the spike protein of the ancestral SARS-CoV-2 (MCMV[S]). In this study, we show that the MCMV[S] elicits a robust and lasting protection in young and aged mice. Notably, S-specific humoral and cellular immunity was not only maintained but even increased over a period of at least 6 months. During that time, antibody avidity continuously increased and expanded in breadth, resulting in neutralization of genetically distant variants, like Omicron BA.1. A single dose of MCMV[S] conferred rapid virus clearance upon challenge. Moreover, MCMV[S] vaccination controlled two immune-evading variants of concern (VoCs), the Beta (B.1.135) and the Omicron (BA.1) variants. Thus, CMV vectors provide unique advantages over other vaccine technologies, eliciting broadly reactive and long-lasting immune responses against COVID-19.

Authors Summary

While widespread vaccination has substantially reduced risks of severe COVID presentations and morbidity, immune waning and continuous immune escape of novel SARS-CoV-2 variants have resulted in a need for numerous vaccine boosters and a continuous adaptation of vaccines to new SARS-CoV-2 variants. We show in proof of principle experiments with a recombinant murine cytomegalovirus expressing the SARS-CoV-2 spike protein (MCMVS) that one immunization with a CMV vaccine vector drives enduring protection in both young and aged mice, with long-term maturation of immune responses that broaden the antiviral effects over time. Hence, this approach resolves issues of immune waning and mitigates the effects of COVID-19 evolution and immune escape, reducing the need for additional immunizations and potentially improving vaccine compliance.

Keywords:

SARS-CoV-2, COVID-19, MCMV, vaccination, single-dose, long-lasting protection, mouse, *in vivo*

Introduction:

The corona-virus disease 2019 (COVID-19), caused by the severe acute respiratory syndrome coronavirus 2 (SARS-CoV-2) (1), had massive impact on public health. The virus rapidly spread across multiple countries in 2020, leading to millions of confirmed cases and deaths in the subsequent years (2). The elderly have been particularly affected by SARS-CoV-2, with a higher risk of severe COVID-19. The exhibited little genetic variation during the early months of the pandemic, with only a single spike substitution (D614G) in the PANGO lineage B.1, which rapidly became dominant in Europe in late 2020 (3). New variants emerged in 2021, characterized by an increasing number of mutations in the spike (S) protein sequence and immune escape potential, including the Beta (B.1.351) (4), the Delta (B1.617.2) (5), or the Omicron variant (B.1.1.529) (6) and its derivatives. Numerous COVID-19 vaccines that induce immune responses against the S glycoprotein have been developed and authorized for use with unprecedented speed. However, vaccine-induced immunity wanes within months, resulting overall in reduced protection against infections and disease (4, 7-9). In addition, emerging variants have been increasingly capable of escaping vaccine-induced immunity driving the need for continued vaccine adaptation and booster shots (10-12). Thus, acute (13) or long-term (14-16) effects after SARS-CoV-2 infection remain a public health issue and a vaccine that confers lasting and broad immune protection remains unmet.

Recently, our research group has demonstrated the capacity of a mouse cytomegalovirus (MCMV)-based COVID-19 vaccine candidate, encoding the S protein derived from the Wuhan prototype (MCMVS), elicits robust and persistent humoral as well as cellular immune responses in mice (17). MCMV is a well-characterized model virus for human CMV (HCMV) infection (18). CMVs are strictly species-specific for their cognate host, and induce robust anti-viral immunity, which persists over a lifetime (19-22). This long-term maintenance of antigen-specific lymphocytes, known as memory inflation (22, 23), is characterized by an accumulation and persistence of CD8 T cells with an effector memory (TEM) phenotype, recognizing immunodominant viral antigens (23, 24). Therefore, transgenic antigens from other infectious agents have been expressed in recombinant MCMVs (25), and such vaccine vectors were shown to provide long-term immune protection (26). This concept was validated in other models of CMV immunization, where a peculiarly strong CD8 T cell immunity was crucial for immune protection (26-31). More recently it was noticed that MCMV infection also results in lasting humoral immune responses toward viral antigens (32), which was exploited to retarget immune protection against other viruses (33), including influenza (17).

90   The S protein of the original strains of SARS-CoV-2 does not bind to mouse ACE2 (mACE2) receptors.
91   Hence, mouse models of SARS-CoV-2 infection were initially restricted to transgenic mice expressing the
92   human ACE2 receptor (hACE2), or mouse-adapted SARS-CoV-2 variants. However, the naturally occurring
93   N501Y mutation in the S protein is sufficient for mACE2 binding (34). Since this mutation was present in
94   various variants of concern (VoCs), including Beta and Omicron, these variants could also be used in
95   infection experiments with non-transgenic mice (35).

96   Here, we show that immunization with MCMV^S elicited virus neutralizing titers (VNTs) that increased for
97   at least 6 months, concomitant with an increase of antibody avidity and resulting in a broadening of
98   neutralization effects to genetically distant variants. The immunization protected vaccinated K18-hACE2
99   mice against lethality and disease manifestations upon challenge with D614G, or Delta VoC. Furthermore,
100   the same vaccination protected BALB/c mice against challenge with the immune-evasive Beta and
101   Omicron strains, and the protection lasted for at least 5 months. Hence, our results argue that CMV-based
102   SARS-CoV-2 vaccines may provide long-term and broad protection against multiple VoCs.

103

104   **Results:**

105   **Protection against SARS-CoV-2 D614G elicited by a single dose of MCMV^S vaccination.**

106   We have previously shown that a single dose of a MCMV-based vaccine vector encoding the S-antigen
107   (MCMV^S) from SARS-CoV-2 triggers a robust inflationary CD8 T cell response against the S-encoded
108   octameric peptide VNFNFNGL in C57BL/6 mice and neutralizing antibody responses which persisted in
109   BALB/c mice for a minimum of 90 days (17). Now we immunized K18-hACE2 mice, which express the
110   human ACE2 receptor (36) and thus may be infected by SARS-CoV-2. We used MCMV^S, a vector control
111   (MCMV^{WT}), or PBS for immunization/mock treatment and challenged the mice with a lethal dose of SARS-
112   CoV-2 B.1 (D614G), 6 or 12 weeks later (Fig. 1A).

113   To quantify the CD8+ T cell response, blood was harvested before the SARS-CoV-2 challenge at 1 or 3
114   months post-immunization, and blood leukocytes were analyzed by flow cytometry (Supplementary Fig.
115   1). MCMV^S and MCMV^{WT} elicited comparable frequencies of CD8 T cells in total, primed, effector (T$_{EFF}$),
116   terminally differentiated effector (T$_{TDE}$), effector memory (T$_{EM}$), and central memory (T$_{CM}$) compartments
117   (Supplementary Fig. 1A). However, only MCMV^S-vaccinated mice displayed high frequencies of
118   VNFNFNGL-specific CD8+ T cells (Supplementary Fig. 1B). The frequency of S-specific T cells was
119   approximately two-fold increased at 3 months over 1 month post-immunization in all tested subsets
120   (Supplementary Fig. 1B) and this was confirmed by dynamic monitoring of S-specific CD8 T cells in the
121   blood (Supplementary Fig. 1C). Likewise, neutralizing titers were typically higher at 3 than at 1 month
122   post-immunization (Supplementary Fig. 1D), in line with our previous report in non-transgenic mice (17).
123   We challenged these mice with $2x10^3$ PFU of SARS-CoV-2 at the indicated time points (Fig. 1A) and
124   monitored weight loss and clinical scores to evaluate protection against COVID-19. Immunized animals
125   that robustly responded to vaccination (Supplementary Fig. 1) were protected against challenge at 6
126   weeks, as evidenced by maintained weight (Fig. 1B) and by the absence of clinical signs (Fig. 1C), while
127   most mock-vaccinated mice became severely ill, reaching the humane end-point by day 5 post-infection
128   (d p.i.) or earlier (Fig. 1D). At 3 and at 5-7 d p.i., MCMV^S vaccination decreased the median SARS-CoV-2
129   viral RNA load in lungs and brains by a factor of 1000 or more relative to mock-vaccinated groups (Fig. 1E-
130   F). The results were similar in the trachea, stomach, heart and spleen (Supplementary Fig. 2A). The
131   immunity of clinically approved vaccines against COVID-19 gradually wanes over time (37, 38). To assess
132   if the protective effects of MCMV^s is reduced over time, mice were challenged at 3 months post
133   immunization. All MCMV^S-vaccinated mice were protected against SARS-CoV-2 infection, in terms of body

134   mass reduction (Fig. 1G), clinical signs (Fig. 1H) and survival (Fig. 1I). Viral RNA burdens were reduced in

135   the MCMV^S-immunized group in all examined organs (Fig. 1 J-K and Supplementary Fig. 2B). Some MCMV^S-

136   vaccinated mice presented viral RNA in lungs at 3 d p.i., but only minor amounts of viral RNAs were

137   detected in this organ at 7 d p.i. (Fig 1J), arguing that a single administration of the MCMV^S vaccine inhibits

138   virus replication. Moreover, the viral RNA load in the brain was ~10,000-fold higher in the controls

139   compared to the MCMV^S immunized mice at day 5-7 post-challenge (Fig. 1K). In sum, single-dose MCMV^S

140   immunization protected animals from COVID-19 at 6 and 12 weeks post-vaccination.
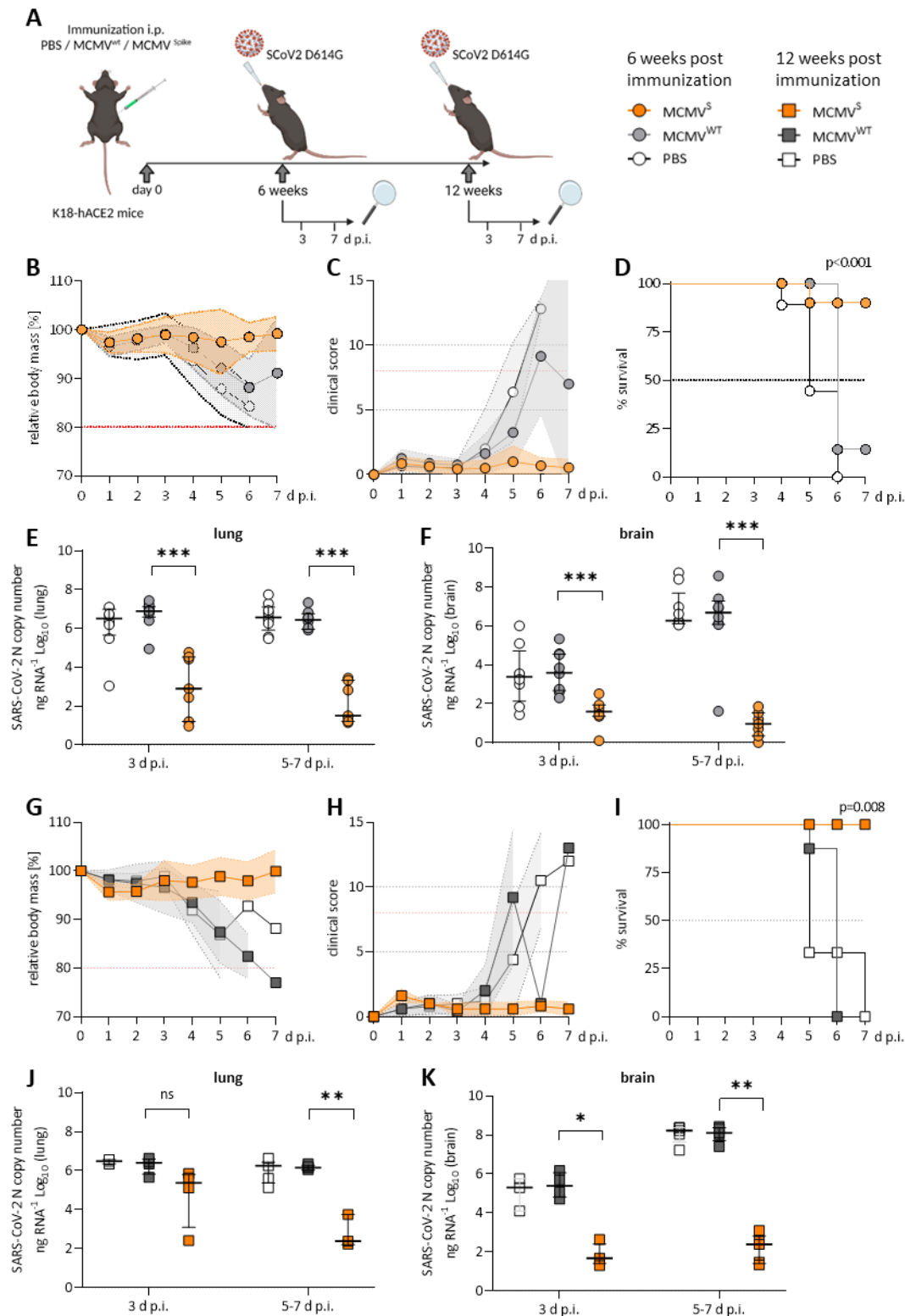
Figure 1: Protection against SARS-CoV-2 D614G elicited by a single dose of MCMV^S vaccination.
(A) Schematic image of the experimental setup and legend for panels B-K. Created with BioRender.com (B-F) Mice were challenged with 2x10^3 PFU of SARS-CoV-2 D614G 6 weeks or (G-L) 12 weeks post immunization. (B, G)

Percentage of body mass relative to day 0 and (C, H) daily clinical scores based on appearance, activity and posture upon challenge are shown. The red dotted line indicates the thresholds resulting in a humane end-point which were used as proxies for survival. (D, I) Mock-survival kinetics of challenged mice representing the Percentage [%] of mice reaching a humane end point. A log-rank (Mantel-cox) test was used for the statistical analysis. (E-F, K-L) SARS-CoV-2 N gene copy numbers as copy number/ng RNA Log10 at 3 d p.i. and 5-7 d p.i. with SARS-CoV-2 D614G in lung homogenates (E, K) and brain homogenates (F, L). Pooled data (n=6-8 per group) from two independent experiments are shown. Statistical significance for was calculated using Welch's t test (two-tailed) (* p < 0.05, ** p <0.01, *** p < 0.001).

141

Sustained neutralizing antibody responses against SARS-CoV-2 Beta and Omicron variants upon MCMV^S immunization

We next tested MCMV^s elicited immunity against the immune evasion Beta (B.1.351) and Omicron (BA.1) VoC. Since both of these VoCs contain the N501Y mutation in the S protein, SARS-CoV-2 infection is possible in non-transgenic mice, such as BALB/c and C57BL/6 (34). The spike used in MCMV^S corresponds to the Wuhan variant of SARS-CoV-2, and therefore does not engage the mACE2 receptor in such mice, potentially resulting in fewer antigen-specific side effects. To assess whether MCMV^S can protect BALB/c in the long term, we challenged mice at five months post-vaccination with the Beta or the Omicron BA.1 variant. A short-term cohort was challenged at 6 weeks after immunization as a point of reference (Fig. 2A). In the short-term cohort, MCMV^S-immunized animals retained their body mass and displayed minimal clinical symptoms, while MCMV^{WT} mock-immunized animals lost approximately 10% of their initial body mass at day three post-infection (Fig. 2B-C). Irrespective of the immunization status, animals that were challenged with the Omicron BA.1 variant showed no reduction in body mass and overall very mild clinical symptoms (Supplementary Fig. 3A-B), in line with reports by other studies.

At five months post-vaccination, MCMV^S-vaccinated animals remained protected against clinical disease upon SARS-CoV-2 Beta challenge (Fig. 2D and E). A randomly selected subset of animals from the long-term cohort was additionally monitored for seven d p.i. for clinical signs and survival. Half of the animals in the mock-immunized group reached the humane end-point, while this occurred in none of the immunized animals (Fig. 2F). Challenge with Omicron BA.1 resulted in no discernible body mass reduction in any of the groups and mild disease in mock-immunized animals 6 weeks (Supplementary Fig. 3A) and 20 weeks post MCMV-immunization (Supplementary Fig. 3B). Altogether, our data indicate that a single dose of MCMV^S vaccination provided a robust and lasting protection against the antigenically distinct Beta variant of SARS-CoV-2, while clinical protection against Omicron BA.1 was hard to assess due to overall low pathogenicity of this variant in mice.

Vaccine efficacy was further assessed by measuring viral RNA copies and infectious titer in the lungs at 3 d p.i.. Both short- and long-term MCMV^S-immunized animals harbored significantly fewer infectious particles in the lungs than the control groups (Fig. 2G). Interestingly, viral RNA load in the short-term immunized cohort was on average slightly higher than in the long-term cohort (Fig. 2H), which might indicate that antiviral activity improved with a longer immunization period. However, three animals in the 20-weeks post-vaccination group showed high viral RNA loads upon infection with the Beta VoC and two of the samples were also highly infectious in terms of PFUs (Fig 2G). In clinical settings, protection against infection and disease of COVID-19 is associated with the presence of neutralizing antibodies (nAb) targeting SARS-CoV-2 (39, 40). Hence, we tested the neutralizing capacity of antibodies targeting different variants of SARS-CoV-2 before and after Beta or Omicron BA.1 challenge. The nAb titers against the Index (Wuhan), Beta and Omicron BA.1 strains were higher at 20-weeks than at 6-weeks post-immunization (Fig. 2I). Importantly, the two immunized mice that showed high infectious virus titers were also the only two mice with undetectable nAb titers (Fig. 2J), indicating that immunization of these animals failed.

179 Importantly, MCMV[S]-vaccinated animals showed a strong capacity to control replication of the
180 antigenically distinct Omicron BA.1 variant. We observed 100-fold reduced viral RNA loads in the short-
181 term cohort and 10,000-fold reduced virus loads in the long-term challenge scenario (Fig. 2K). Infectious
182 Omicron BA.1 virus remained undetectable in any scenario (data not shown).
183 Collectively, a receptor-inert S antigen delivered through an MCMV-based vector prompted robust and
184 persistent nAb reactions, with no signs of immune waning and predictively correlated with a decrease in
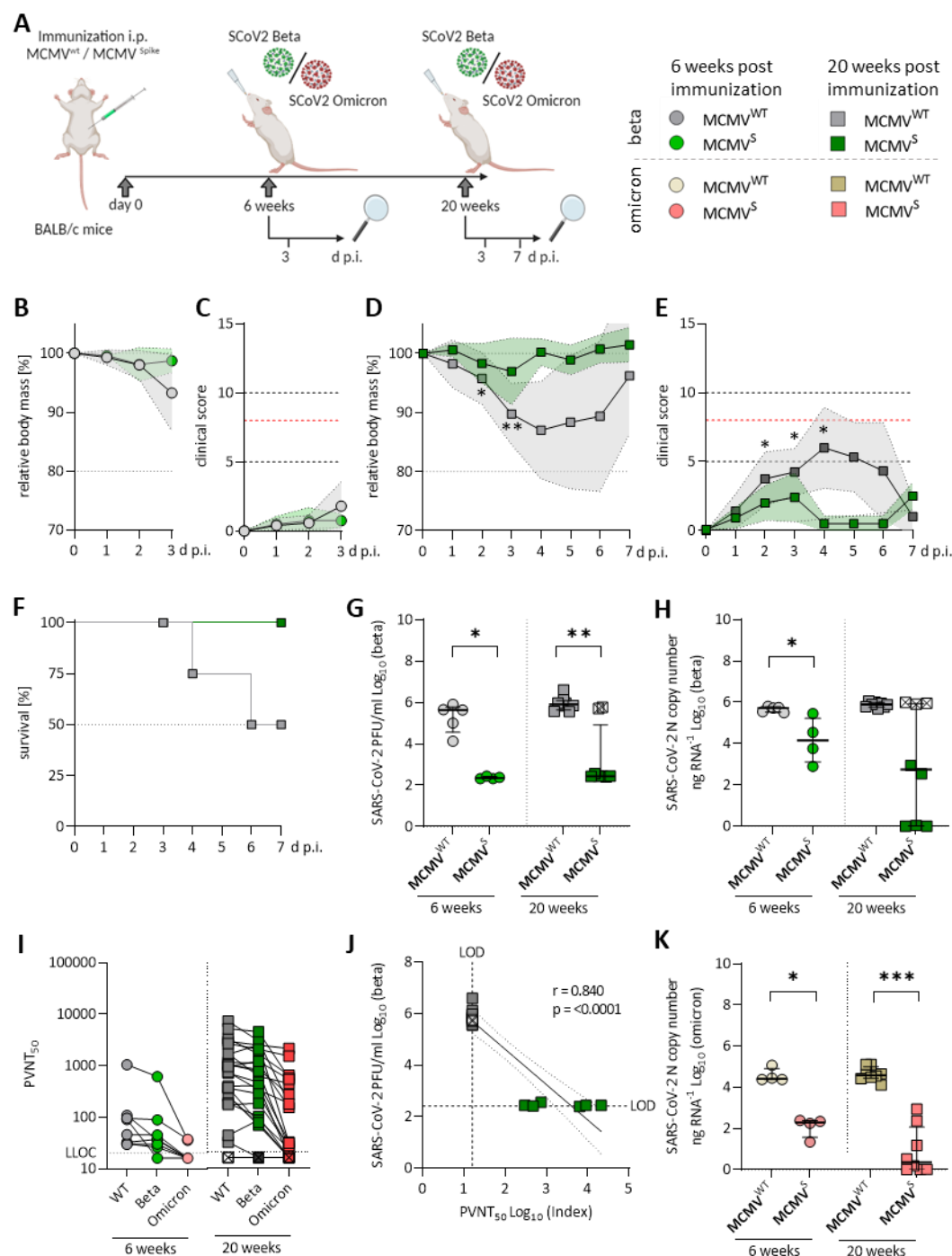185 SARS-CoV-2 viral titers upon challenge.

Figure 2: Sustained neutralizing antibody responses against Beta and Omicron BA.1 variants upon MCMV^S immunization. *(A) Schematic image of the experimental setup and legend. Mice were challenged with 6x10^4 PFU of SARS-CoV-2 in all settings. Created with BioRender.com. (B, C) Mice were challenged at 6 weeks after immunization. Relative body mass (B) and clinical scores (C) were monitored daily upon challenge with the Beta variant. (D-F) Mice were challenged with SARS-CoV-2 Beta 20 weeks after immunization. (D) Percentage of body mass, (E) daily clinical scores and (F) survival kinetics of challenged mice represented as the percentage of mice reaching the humane end point due to a high clinical score. The threshold resulting in this humane end-point is indicated by the red dotted line in panel (E). (G) Infectious virus titers in lungs of SARS-CoV-2 Beta-challenged mice 6 weeks (left) and 20 weeks (right) post immunization. (H) Relative viral RNA loads in lungs of SARS-CoV-2 Beta-challenged mice normalized to GAPDH. (J) Pseudovirus serum neutralization titers resulting in a 50% reduction of SARS-CoV-2 infection (PVNT$_{50}$). PVNT$_{50}$ at 6 weeks (n=8; left) and 20 weeks (n=24; right) post-vaccination against the Index (Wuhan), Beta and Omicron BA.1 variants. Titers were assessed seven days before SARS-CoV-2 challenge. Dot plots representing the same mice are connected by lines. Solid horizontal lines show the median and the dotted line indicates the detection limit. (J) Correlation of Infectious virus titers in lungs and PVNT50 against the Index strain of SARS-CoV-2 Beta-challenged mice after 20 weeks post immunization. (K) Relative viral RNA loads in lungs of SARS-CoV-2 Omicron BA.1-challenged mice normalized to GAPDH. Statistical significance for was calculated using Welch's t test (two-tailed) (* p < 0.05, ** p <0.01, *** p < 0.001).*

186

Single-dose of MCMV^S provides inflationary immunogenicity in aged mice

187
188 The elderly population is of special concern when it comes to COVID-19, due to their increased
189 vulnerability and diminished vaccine efficacy. Hence, we assessed the potential of MCMV^S-based vaccines
190 in aged hosts. Specifically, we immunized aged K18-hACE2 mice at 14-16 months of ageeither with MCMV^S
191 or the MCMV^{WT} as control vector (Fig. 3A). The neutralization capacity of sera was examined before SARS-
192 CoV-2 challenge at 6 and 12 weeks, as well as up to 24 weeks postimmunization. Virus-nAb titers increased
193 over time, albeit this increase was not significant for the Index or the Beta variant (Fig. 3B). Only a few
194 mice showed detectable titres of neutralising antibodies against Omicron BA.1 or BA.4/5 shortly after
195 immunization. However, cross-reactive titers against these variants increased significantly over time
196 against both Omicron , with approximately half of the animals exhibiting robust titers 6 months post-
197 vaccination (Fig. 3B).

198 After repeated antigen exposure, B cells undergo somatic hypermutation and affinity maturation
199 processes, yielding high-affinity antibodies that efficiently bind to antigens, in our case SARS-CoV-2 S (41-
200 43). Thus, re-exposure of primed B cells to the antigen improves virus neutralization efficacy due to affinity
201 maturation. Since MCMV-based vaccines stimulated robust antibody responses with increasing
202 neutralization capacity (17), we considered that these functional responses may be driven by affinity
203 maturation, or by polyclonal B-cell expansion and a pure increase in antibody titers. Hence, we quantified
204 SARS-CoV-2 S-specific total IgG levels upon vaccination over time (Fig 3C). Kinetic measurements revealed
205 no significant differences in total IgG levels, against both the Index and the Omicron BA.1 variant (Fig. 3C).
206 Serum samples from control mice that underwent mock immunization were typically below the detection
207 threshold (data not shown). We next tested IgG binding avidity by exposing sera to various concentrations
208 of sodium thiocyanate (NaSCN), as described previously (17). We observed an increase in avidity over
209 time, from 6 and 12 to 24 weeks post-immunization (Fig. 3D). Consistent levels of total anti-S IgG alongside
210 a concurrent rise in binding affinity within the same sera may indicate that the increase in neutralization
211 was driven primarily by affinity maturation.

212 To identify the limits of our vaccine approach, we subjected it to a stress-test, where we analysed long-
213 term immunity upon a vaccine dose that was 5-fold lower than in previous experiments. At 16 months
214 post-immunization, spike-specific splenic CD8 T cells were detectable at sustained levels, with a median
215 frequency of 10% of VNF-specific cells in the CD8 population (Supplementary Fig. 4A), and a predominant

216 effector phenotype (Supplementary Fig. 4B). Furthermore, some mice still harboured nAb against SARS-
217 CoV-2, including the BA.4/5 variant (Supplementary Fig. 4C), while anti-spike IgG could be observed by
218 ELISA (Supplementary Fig. 4D). Thus, a single dose of the MCMV^S-based vaccine provided lasting,
219 potentially lifelong, humoral and cellular immunity in aged mice.
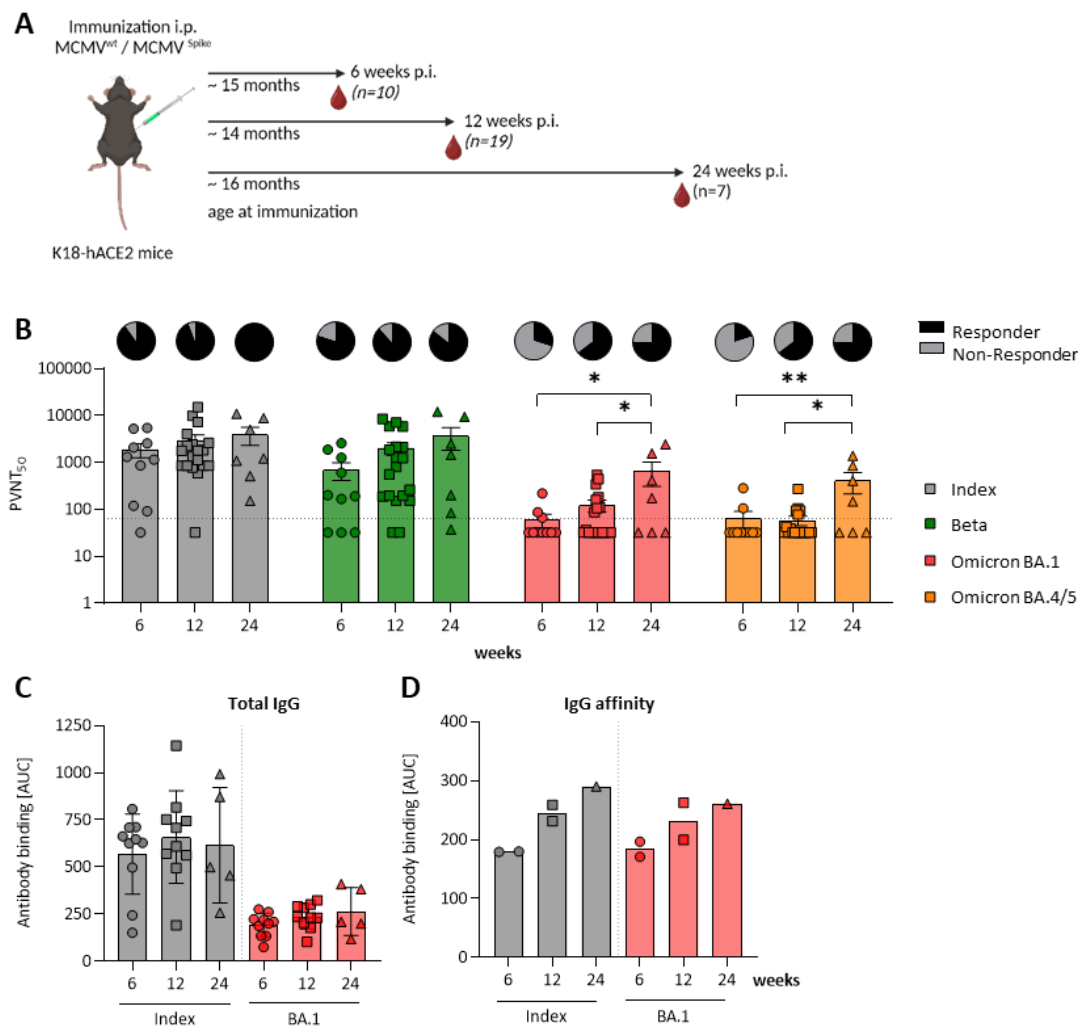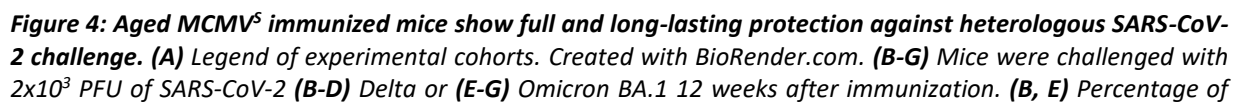220

Figure 3: A single-dose of MCMV^S provides inflationary immunogenicity in aged mice. *(A) Schematic image of the experimental setup. Created with BioRender.com. (B) Pseudovirus neutralization titers that resulted in a 50% of reduction of SARS-CoV-2 infection (PVNT$_{50}$). Sera of 6 (n=10), 12 (n=19) and 24 (n=7) weeks MCMV^S-immunized mice were tested against the Index (Wuhan; grey), Beta (blue), Omicron BA.1 (red) and Omicron BA.4/5 (orange) SARS-CoV-2 strains. Each symbol indicates an individual mouse. Solid horizontal lines show the median and the dotted line indicates the detection limit. Pie charts indicate the percentage [%] of animals, that responded (black) or non-responded (grey) with nAb titers. (C-D) SARS-CoV-2 Spike specific IgG response against the Index and Omicron BA.1 variants in murine sera after 6, 12, and 24 weeks post-immunization. (C) Total IgG and (D) IgG affinity measured by antibody binding [AUC] in presence of graded amounts of NaSCN using ELISA. Statistical significance for was calculated using Welch's t test (two-tailed) (* p < 0.05, ** p <0.01).*

221
222

223 **Aged MCMV^S immunized mice show full and long-lasting protection against heterologous SARS-CoV-2**
224 **challenge**

225 We subsequently assessed the immune protection provided to aged mice by a single-dose MCMV^S
226 vaccination. We challenged aged K18-hACE2 mice with two SARS-CoV-2 variants. Mice were infected with
227 2×10^3 PFU of SARS-CoV-2 Delta or Omicron BA.1 at 6 or 12 weeks post-immunization (Fig. 4A). Mice
228 immunized with MCMV^S were fully protected against body mass loss (Fig. 4B) and clinical manifestations
229 of disease (Fig. 4C) for up to 12 weeks post-immunization when challenged with the virulent Delta variant,
230 while mock-vaccinated mice exhibited severe illness and approximately half among them reached the
231 humane end-point by day five post-infection (Fig. 4D). Mice challenged with the Omicron BA.1 variant
232 demonstrated overall minimal body mass loss (Fig. 4E) and exhibited only mild clinical symptoms (Fig. 4F),
233 irrespective of immunization status, consistent with our previous findings (Fig. 2). Moreover, protection
234 against body mass reduction (Supplementary Fig. 5A) and clinical signs (Supplementary Fig. 5B) was
235 observed in animals challenged 6 weeks after MCMV^S immunization when compared to MCMV^{WT}-controls
236 and they consistently survived (Supplementary Fig. 5C). Vaccine efficacy was further evaluated by
237 quantifying the viral RNA burden (Fig. 4H) and infectious titers in the lungs (Fig. 4I) and brain (Fig. 4J) at
238 five d p.i.. Analyses of viral load in SARS-CoV-2 Delta-challenged mice revealed a >1000-fold reduction in
239 lungs (Fig. 4H, *top*) and brains (Supplementary Fig. 5D) in immunized animals. We also observed a marked
240 (~100-fold) reduction of SARS-CoV-2 viral RNA in lungs (Fig. 4H, *bottom*) of mice challenged with the
241 Omicron variant, while brains showed low levels of Omicron mRNA, even in mock-vaccinated mice
242 (Supplementary Fig. 5E).
243 MCMV^S immunized mice harbored no detectable infectious virus particles in lungs (Fig. 5I) and brains (Fig.
244 5J) at five days post challenge, indicating efficient and fast clearance in immunized animals. Taken
245 together, MCMV^S fully protected aged mice against SARS-CoV-2 Delta challenge up to three months post-
246 vaccination and reduced viral loads of the Delta and the antigenically distinct Omicron BA.1 variant.
247

Figure 4: Aged MCMV^S immunized mice show full and long-lasting protection against heterologous SARS-CoV-2 challenge. (A) *Legend of experimental cohorts. Created with BioRender.com.* **(B-G)** *Mice were challenged with 2x10^3 PFU of SARS-CoV-2* **(B-D)** *Delta or* **(E-G)** *Omicron BA.1 12 weeks after immunization.* **(B, E)** *Percentage of*

*initial body mass and **(C, F)** daily clinical scores upon challenge are shown. The red dotted line indicates the threshold in score resulting in a humane end-point. **(D, G)** Survival kinetics of challenged mice representing the Percentage [%] of mice reaching a humane end point. A log-rank (Mantel-cox) test was used for the statistical analysis. **(H)** SARS-CoV-2 N gene copy numbers as copy number/ng RNA Log10 at 5 d p.i. with SARS-CoV-2 Delta (top) or Omicron BA.1 (bottom) in lung homogenates **(I-J)** Infectious virus titers in **(I)** lungs and **(J)** brains of SARS-CoV-2 Delta-(top) or Omicron BA.1 (bottom) challenged mice. Statistical significance was calculated using Welch's t test (two-tailed) (* p < 0.05, ** p <0.01, *** p < 0.001).*

248

249 **MCMV^S protects against subclinical inflammation following Omicron BA.1 infection.**

250 We used bulk RNA sequencing to investigate gene expression patterns associated with inflammation in
251 lung samples after challenge with both Delta and Omicron variants in our long-term vaccination cohort.
252 We observed a consistent difference in expression levels of genes involved in pathogen response and
253 inflammation between the vaccinated mice and their mock vaccinated controls. The expression of genes
254 related to interferon-gamma (IFNγ) and the type I interferon response, as well as Interferon (IFN)
255 signalling cascade were clearly reduced in vaccinated mice upon both Delta and Omicron challenge (Fig.
256 5A). These data were in line with the reduction in symptoms observed upon Delta challenge and indicated
257 that Omicron BA.1 infection induces a sub-clinical inflammation in mice, which was clearly reduced
258 following vaccination. Cytokines that play crucial roles in inflammatory processes and are suspected to
259 contribute to immunopathology were analyzed in more depth. Several among them including IL-6,
260 CXCL10, IL15 or LIF were significantly elevated in the mock- compared to the MCMV^S-vaccinated animals
261 after SARS-CoV-2 Delta (Fig. 5B, left) and Omicron BA.1 (Fig. 5B, right) challenge. As expected, expression
262 was higher among the animals challenged with the Delta variant, than the Omicron, among mock-
263 immunized animals. While expression was similarly reduced among MCMV^{S-}immunized mice. Contrarily
264 to inflammatory markers, T cell markers associated with the activation, differentiation, proliferation, and
265 memory formation of T-cell responses post-vaccination were up-regulated in MCMV^S immunized mice
266 compared to their controls upon Delta and Omicron BA.1-infection (Fig. 5C). In summary, our findings
267 indicate that vaccination with MCMV^S not only leads to a strong immune response but also protects
268 against sub-clinical inflammation caused by the antigenically distinct Omicron variant.
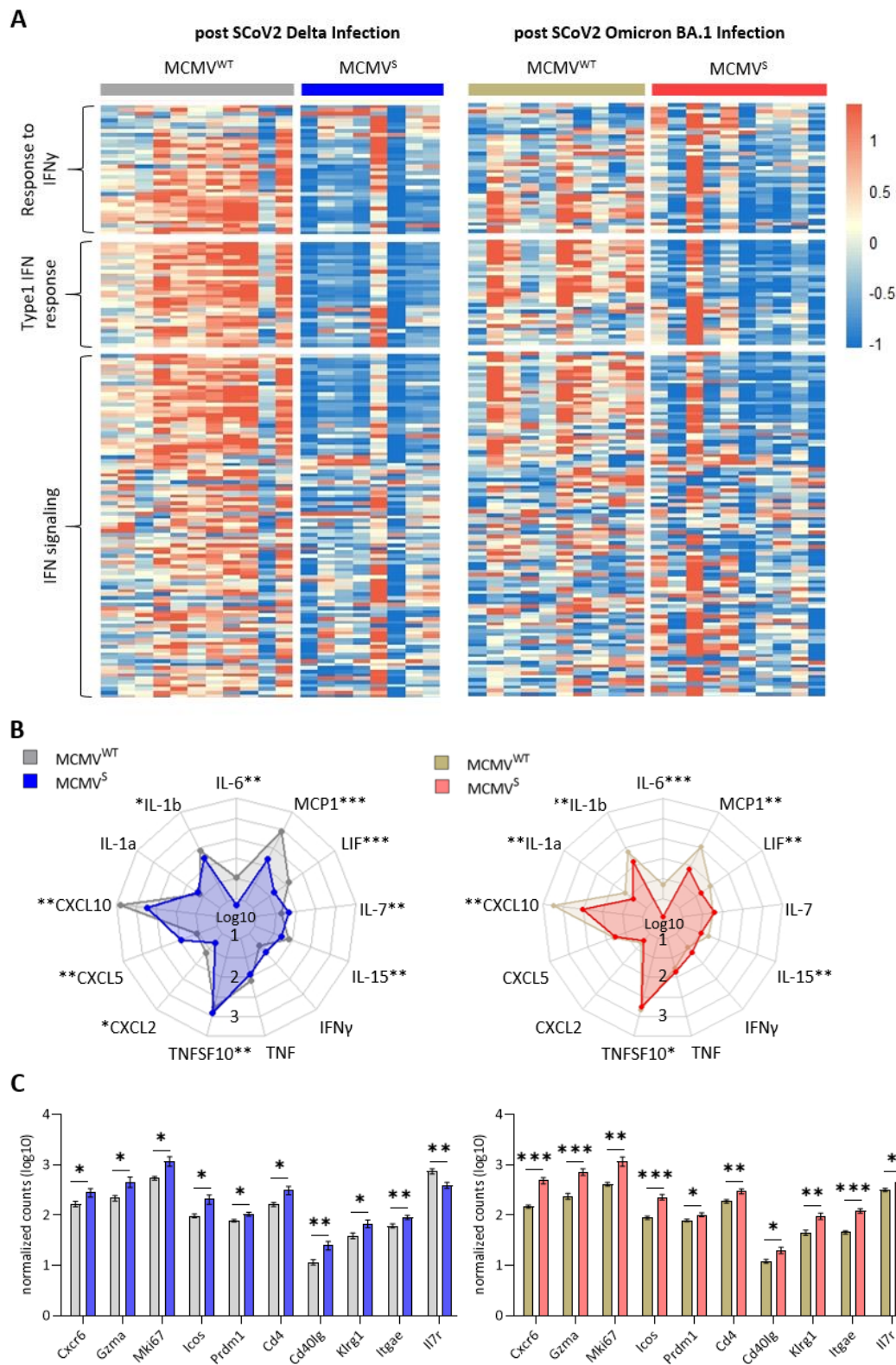
269

270

Figure 5: MCMV^S shows efficacy against the subclinical inflammation progression of Omicron BA.1. (A) *Heat maps of differently expressed genes in response to vaccination involved in the response to IFNy, type 1 IFN response and related to IFN signaling (44). Differentially expressed genes of mice infected with the Delta (left) or*

*Omicron variant (right) of SARS-CoV-2 and vaccinated with the MCMV^WT or S-modified MCMV vaccine was performed after bulk RNA sequencing of the lung tissue. Columns represent different animal samples and rows, genes. Shown are z-scores of DESeq2-normalized data and color scale ranges from red (10 % upper quantile) to blue (10 % lower quantile), showing up- or downregulation in expression of the selected genes, respectively. **(B)** Spider plot of differentially expressed cytokines between the 2 vaccine strategies. Values are DESeq2-normalized data in a log10 scale represented for each gene analyzed. **(C)** Heat map of differentially expressed genes involved in T cell activation and proliferation (45). Shown are z-scores of DESeq2-normalized data and color scale ranges from red (10 % upper quantile) to blue (10 % lower quantile), showing up- or downregulation in expression of the selected genes, respectively. N = 8-11 animals per group. (D) Cell-type deconvolution of bulk RNA-Sequencing performed with GEDIT for cell type prediction based on blood reference matrix provided by the program. Shown are fractions of the cell type selected of the total count.*

271

272 **Discussion:**

273 Several vaccines have been developed to combat the COVID-19 pandemic. Nevertheless, immune waning
274 remains an unresolved challenge (6-8, 46), and vaccines resulting in lasting and broad protection against
275 SARS-CoV-2 variants remain unavailable. Viral vectors that were authorized early in the COVID-19
276 pandemic, such as Vaxzevria (ChAdOx1-S) and the COVID-19 vaccine from Janssen (Ad26.COV2.S) (47, 48),
277 provide immune protection that is relatively short-lived, which also afflicts the mRNA-based vaccines (49).
278 CMV has received attention as a potential vaccine vector tool because it induces strong and lasting T-cell
279 immunity (26). While HCMV seroprevalence is estimated to exceed 90% in some geographic areas, the
280 pre-existing immunity to CMV does not hinder vaccine responses and protection in studies with rhesus
281 monkeys (27, 50), arguing that CMV vectors may be used in CMV seropositive populations. MCMV shares
282 structural and functional homologies with HCMV and allows *in vivo* analyses in the natural host. We show
283 here, using the murine CMV vaccine vector model, that CMV-based vectors provide durable and
284 protective immunity upon a single immunization. Hence, our data may indicate that a CMV based vaccine
285 may provide durable and broad immune protection against COVID-19.

286 Neutralizing antibody responses correlate with vaccine effectiveness (51) and MCMV^S elicits strong
287 neutralizing antibody responses whose affinity and neutralizing capacity increase over time (17). Here, we
288 show that MCMV^S induces antibodies that neutralize the antigenically distinct Beta and Omicron variants
289 and protect against disease upon infection with these viruses, with neutralization titers increasing for at
290 least 6 months post-vaccination (Fig. 3B; 2J). This feature is unique for this vector and superior to other
291 vaccine formulations, which require repeated booster administrations to avoid immune waning over time
292 (47, 48, 52, 53). Considering that neutralizing antibodies against SARS-CoV-2 wane at similar rates upon
293 infection or vaccination with currently used vaccines (9, 46, 54-56), our vaccine might provide an immunity
294 that is even better than that induced by infection.

295 Interestingly, even the relatively weak neutralizing antibody responses against the SARS-CoV-2 Omicron
296 variant were associated with protection against illness and lowered viral loads in the lungs (Fig. 2). One
297 may speculate that T cell immunity elicited by MCMV^S vaccination protected these animals. Similar
298 phenomena were documented in preclinical studies with rhesus macaques or in clinical studies, where
299 study subjects were protected although no neutralizing antibodies were observed (57-59). However, we
300 cannot exclude the possibility that memory B lymphocytes in MCMV^S-immunized mice responded to the
301 challenge by rapidly generating neutralizing antibodies upon challenge, thus limiting virus replication and
302 protecting the host. Finally, it may also be possible that the concerted action of these two lymphocyte
303 lineages protected the vaccinated mice against challenge. To differentiate between these scenarios, one
304 may use MCMV vectors eliciting only T cell responses against S epitopes, or mice lacking T cells. However,
305 such experiments would go beyond the scope of this study.

306 In this study, we showed that even an S antigen that cannot bind to the target ACE2 receptor in vaccinated
307 subjects may still provide robust immune protection. Namely, the S antigen from the prototypical Wuhan
308 strain of SARS-CoV-2, which was cloned into our vaccine vector, cannot bind to the murine ACE2 receptors
309 (60). Nevertheless, MCMV^S protected BALB/c mice against variants that encode an N501Y mutation and
310 thus engage the mACE2 and may replicate in mice. Some studies reported that the binding of the S1
311 subunit of the S protein to ACE2 on endothelial cells may affect endothelial barrier integrity and cardiac
312 activity (61-63), which would be excluded in such approaches. While we observed no adverse effects in
313 hACE2 mice immunized in the long term with our vector, arguing against such adverse effects (or other
314 side effects, unrelated to ACE2 biding), our data demonstrate that spike formulations may protect against
315 SARS-CoV-2 infection in absence of ACE2 receptor engagement by the vaccine-encoded spike, which was
316 a concern in light of low levels of S antigen persistence in the host.
317 With this study we clearly show that even in Omicron infected mice, which do not display overt disease
318 pathogenesis, sub-clinical inflammation is reduced by an MCMV vector encoding an antigenically distinct
319 spike variant (Fig 4-5). However, Bulk RNA sequencing in inflammation research involves analyzing a mixed
320 population of cells together, providing only a snapshot of the average genetic expression. Hence, our
321 analysis may help to identify gene expression patterns associated with inflammation across a tissue
322 sample, but it lacks the ability to pinpoint specific cellular contributions to gene expression profiles. Single-
323 cell sequencing offers a more detailed view of individual cell responses in inflammation studies, allowing
324 for a deeper understanding of cellular heterogeneity and potential therapeutic targets. Such analysis may
325 be performed in the future to better understand the mechanisms by which immunization prevents hyper-
326 inflammatory responses to infection.
327 The data presented here demonstrate that an MCMV-based vaccine candidate expressing the full-length
328 prototype S protein is highly immunogenic and protective in mice. We demonstrated that a single dose of
329 the MCMV^S may protect not only young, but also aged mice against a lethal dose of the SARS-CoV-2, and
330 that the protection acts against immune-evasive Beta and Omicron variants. Our approach provided
331 evidence for lifelong immunity, especially in terms of T cell responses. Future research needs to focus on
332 a head-to-head comparison of MCMV-based vaccines with other COVID-19 vaccine formulations, on the
333 length of protection and administration routes, paving the way towards clinical trials with CMV vectors.
334 We propose a radical departure from the conventional vaccines against COVID-19 that provide only short-
335 term protection that require continuous boosters and frequent adaptations of the antigen in the vaccine
336 to circulating spike variants. This study demonstrates that in principle, such approach is feasible.
337

338 **Material and Methods:**
339 *Cell culture and viruses*
340 Vero E6 (CRL-1586) and M2-10B4 cells (ATCC CRL-1972) were cultured as described previously (17). Caco-
341 2 cells (ACC 169) were purchased from DSMZ (Braunschweig, Germany) and were cultured in DMEM
342 (Gibco, NY, USA) supplemented with 20% fetal bovine serum (FBS), 2 mM L-glutamine, 100 IU/mL
343 penicillin and 100 μg/mL streptomycin. The FI strain of SARS-CoV-2 (GISAID database ID: EPI_ISL_463008)
344 was described previously as a D614G variant (64) and was passaged on Caco-2 cells in the biosafety level
345 3 (BSL3) laboratory at HZI. A clinical isolate of the SARS-CoV-2 B.1.617.2 (Delta) variant was isolated at the
346 Fran Mihaljevic clinical center in Zagreb and propagated as previously described (64).
347 SARS-CoV-2 genome sequences are available on GISAID and GenBank under the following accession
348 numbers: SARS-CoV-2 B.1.351 (Beta) FFM-ZAF1/2021 (GenBank ID: MW822592) (65) and SARS-CoV-2
349 B.1.1.529 (BA.1) FFM-ZAF0396/2021 (EPI_ISL_6959868; GenBank ID: OL800703) (66). MCMV^{WT} refers to
350 the BAC-derived molecular clone of MCMV (pSM3fr-MCK-2fl clone 3.3) (67). MCMV^S was generated by *en*

351 *passant* mutagenesis, as described previously (17). Briefly, the codon-optimized S protein of the Wuhan
352 variant replaced the coding sequence of the viral ie2 protein.
353 The expression vector for SARS-CoV-2 S protein of Omicron (BA.1) (based on isolate hCoV-
354 19/Botswana/R40B58_BHP_3321001245/2021; GISAID Accession ID: EPI_ISL_6640919), BA.4/5 (based on
355 isolate hCoV-19/England/LSPA-3C01A75/2022 was generated by Gibson assembly as described previously
356 (68) and then subsequently introduced in pseudotype VSV backbone that lacks VSV glycoprotein G (VSV-
357 G) (69). A plasmid encoding the S protein of SARS-CoV-2 Beta (B.1.351) has been previously reported (17).
358

Virus stock generation and plaque assay
360 BAC-derived MCMV was reconstituted by transfection of BAC DNA into NIH-3T3 cells (ATCC CRL-1658)
361 using FuGENE HD transfection reagent (Promega, WI, USA) according to the manufacturer's instructions.
362 Transfected cells were cultured until viral plaques appeared and passaged 5 times in M2-10B4 cells before
363 virus stock production. Virus stocks were prepared on ice. First, supernatants of infected M2-10B4 cells
364 were collected and infected cells were pelleted (5,000 × g for 15 min). The resulting cell pellets were
365 homogenized in DMEM supplemented with 5% FBS and cell debris was removed by centrifugation (12,000
366 x g for 10 min). Collected supernatants were resuspended in VSB buffer (0.05 M Tris-HCl, 0.012 M KCl, and
367 0.005 M EDTA, adjusted to pH 7.8) and then concentrated by centrifugation through a 15% sucrose
368 cushion in VSB buffer (23,000 × g for 1.5 h). The resulting pellet was resuspended in 1-1.5 mL VSB buffer,
369 briefly spun down, and supernatants were aliquoted and kept at -80˚C. BAC-derived mutant MCMV^S were
370 propagated on M2-10B4 cells and concentrated by sucrose density gradient centrifugation.
371 SARS-CoV-2 D614G was generated and viruses were quantified by plaque assays as described before (17)
372 with a minor modification that Caco-2 cells were used for virus production. SARS-CoV-2 Beta, Delta and
373 Omicron BA.1 stocks were generated as described previously and titers were determined by the median
374 tissue culture infective dose (TCID50) method (66).
375 Pseudotyped viruses were harvested as described before (17, 68). In brief, 293T cells were transfected
376 with expression plasmids (pCG1) encoding different S proteins of SARS-CoV-2 variants by using the
377 calcium-phosphate method. At 24h post-transfection, the medium was removed and cells were
378 inoculated with a replication-deficient VSV vector lacking its glycoprotein and coding instead for an
379 enhanced green fluorescent protein (GFP) (kindly provided by Gert Zimmer, Institute of Virology and
380 Immunology, Mittelhäusern, Switzerland). Following 1 h incubation at 37°C, the cells were washed with
381 PBS, and culture media containing anti-VSV-G antibody (culture supernatant from I1-hybridoma cells;
382 ATCC CRL-2700) were added. The pseudotype virus was harvested at 16-18 h post-infection.
383

Virus in vivo infection
385 K18-hACE2 mice were obtained from Jackson Laboratories and bred in the core animal facility of
386 Helmholtz Center for Infection Research, Braunschweig. BALB/c mice were purchased from Envigo (IN,
387 USA). All animals were housed under Specific Pathogen Free (SPF) conditions at HZI during breeding and
388 infection. All animal experiments were approved by the Lower Saxony State Office of Consumer Protection
389 and Food Safety, license number: 33.19-42502-04-20/3580.
390 K18-hACE2 mice (2-6 months old and >17 months) were intraperitoneally (i.p.) immunized with 10^6 PFU
391 of recombinant MCMV^S or MCMV^{WT} diluted in PBS or treated with PBS (200 µl i.p. per animal). BALB/c
392 mice (4-7 months old) were i.p. immunized with 2x10^5 PFU of recombinant MCMV^S or MCMV^{WT}. All mice
393 were weekly or bi-weekly monitored and scored for their health status after vaccination. Blood was
394 isolated at indicated time points by puncture of the retrobulbar plexus or by cardiac bleeding upon death.
395 SARS-CoV-2 challenge experiments were performed in the HZI BSL3 laboratory essentially as described
396 (70) with the following modifications: K18-hACE2 mice were intranasally (i.n.) infected with 2x10^3 PFU of

397 D614G, Delta or Omicron BA.1 SARS-CoV-2 variant, while BALB/c mice were challenged with $6x10^4$ PFU of
398 the VoCs. SARS-CoV-2-infected mice were monitored for body mass loss and clinical status at least daily,
399 according to the animal permit.
400 SARS-CoV-2-challenged animals were scored daily to monitor any signs of disease development. Animals
401 were scored based on five criteria: spontaneous/social behaviour, fur, fleeing behaviour, posture, and
402 body mass loss. Each score indicates the following: no signs of symptoms (score=0), mild and/or sporadic
403 symptoms (score=1), moderate and/or frequent symptoms (score=2), and severe symptoms with a clear
404 sign of heavy suffering (score=3). Weight loss criterion is scored as follows: ≤1 % (score=0), 1-10 %
405 (score=1), 10-20% (score=2), and >20% (score=3). Mice with a score of 3 in one criterion, or an overall
406 score of ≥9, were removed from the experiments.
407
408 ***Organ harvest***
409 Animals were euthanized by CO_2 inhalation, blood was collected from the heart and kept at room
410 temperature (RT) for 30–60 min until clotting occurred, then stored at 4 °C. For further analysis, serum
411 was isolated by centrifugation. The trachea, lungs, heart, spleen, stomach, and brain were harvested at 3,
412 5 or 7 days post-SARS-CoV-2 challenge. In animals that reached humane endpoints before 7 days post-
413 challenge, organs were harvested on the day of euthanasia. Solid organs were weighed and homogenized
414 in bead-containing lysis tubes (Lysis tube E, Analytik Jena) in 500 µL or 1,000 µL PBS with an MP Biomedical
415 FastPrep 24 Tissue Homogenizer (MP Biomedicals, CA, USA) (full speed, 2 × 20 s) and stored at -80°C.
416 Samples designated for RNA-isolation or bulk sequencing were mixed with Trizol reagent (Invitrogen) at a
417 1:3 ratio. All centrifugation steps were carried out at 10,000× g for 10 min at 4 °C.
418
419 ***RNA isolation and viral loads analyses***
420 RNA isolation was performed with the Rneasy RNA isolation kit (Quiagen) or innuPrep Virus TS RNA kit
421 (Analytik Jena), according to the manufacturer's protocol. Shortly, for the first experiments of infected
422 K18-hACE2 mice challenged with D614G the Rneasy RNA isolation kit was used by adding 250 µL of organ
423 homogenates in 750 µL Trizol and subsequently centrifuged at 16,000 x g for 3 min. The resulting
424 supernatants were carefully collected and washed with the same volume of 70% Ethanol. The mixed
425 solution was transferred into a collection tube and centrifuged at 10,000 x g for 30 sec. After decanting
426 the flow-through, the column was washed once with 700 µL of RW1 wash buffer and twice with 500 µL
427 RPE buffer. Lastly, 40 µL of nuclease-free water was added to the column for RNA elution. For the
428 remaining experiments including the BALB/c and K18-hACE2 mice challenged with the SARS-CoV-2 VoCs
429 RNA extraction was conducted using the innuPrep Virus TS RNA kit (Analytik Jena) following the
430 manufacturer's instructions. In brief, Trizol-inactivated samples were combined with an equal volume of
431 lysis solution CBV, which contained carrier RNA and Proteinase K. This mixture was then incubated at 70
432 °C for 10 minutes. After the lysis step, samples were blended with two sample volumes of isopropanol.
433 Subsequently, the samples were applied to the provided spin filters, washed with washing buffer (LS), and
434 rinsed with 80% ethanol. RNA was finally eluted in 60 µL of RNase-free water and stored at -80 °C after
435 determining the RNA concentration using a NanoDrop (Thermo Scientific NanoDropOne).
436 Eluted RNAs were analyzed further to assess viral RNAs in the given organs by quantitative reverse
437 transcription polymerase chain reaction (RT-qPCR). The reaction was performed with a total volume of 20
438 µL containing 2 µL of sample RNAs or positive control RNAs, 5 µL TaqPath 1-step RT-qPCR Master Mix with
439 ROX reference dye, and 1.5 µL probe/primer sets. 2019-nCoV RUO kit was used to detect SARS-CoV-2
440 RNAs (Integrated DNA Technologies (IDT), USA), and Taqman Rodent GAPDH control reagents
441 (ThermoFischer Scientific, USA) were used for endogenous GAPDH RNAs. For absolute viral RNA

442   quantification, a standard curve was generated by serially diluting a SARS-CoV2 plasmid with the known
443   copy numbers 200,000 copies/µL (2019-nCoV_N_Positive Control, #10006625, IDT, USA) at 1:2 ratio in all
444   PCR analyses, with a quantitation limit of 20 copies of the plasmid standard in a single qPCR reaction. The
445   viral RNA of each sample was quantified in triplicate and the mean viral RNA was calculated by the
446   standard. RT-qPCR was performed using the StepOnePlusTM Real-Time PCR system (ThermoFischer
447   Scientific, USA) according to the manufacturer's instructions. SARS-CoV-2 N-gene copy numbers were
448   normalized to total RNA input and to rodent GAPDH copy numbers.
449

Detection of infectious SARS-CoV-2 titers by plaque assay

451   Lung and brain organ homogenates were serially diluted in DMEM (Gibco, NY, USA) supplemented with
452   5% FBS and 100 IU/mL penicillin, and 100 µg/mL streptomycin. 100 µL of sample dilutions were
453   transferred onto confluent VeroE6 cells in a 96-well format. After inoculation for 1 h at 37 °C, the inoculum
454   was removed and 1.5% methylcellulose in MEM supplemented with 5% FBS, 2 mM L-glutamine, 100 IU/mL
455   penicillin, and 100 µg/mL streptomycin was added to the cells. The infected cells were incubated at 37 °C
456   for 48 h before inactivation with a 4% formalin solution in PBS for 10 min at RT. The fixed cells were
457   subjected to immunofluorescent staining against the SARS-CoV-2 N protein. Briefly, fixed cells were
458   permeabilized with 0.1% Triton X-100 (Sigma-Aldrich, MA, USA) for 10 min at RT and blocked with 1% BSA
459   (Sigma-Aldrich, MA, USA) in PBS for 30 min at RT. Thereupon, cells were incubated with a monoclonal
460   anti-SARS-CoV-2 N protein antibody (Abcalis, AB84-E02, 10 µg/mL) for 30 min at RT. After washing three
461   times with PBS with 0.05% Tween-20 (PBS-T), a secondary antibody anti-mouse IgG conjugated with
462   Alexa488 (Cell Signaling Technology, #4408, 1:500) was added for 30 min at RT. After washing three times
463   with PBS-T, the stained cells were visualized using Incucyte S3 (Sartorius; GUI software versions 2019B
464   Rev1 and 2021B).
465

Flow cytometry quantification of S-specific T cells

467   Peripheral blood was harvested and red blood cells were removed by short osmotic shock. Thereupon,
468   lymphocytes were stained with S-derived VNFNFNGL-specific tetramers (Kindly provided by Ramon Arens,
469   Leiden University) for 30 min at RT. Subsequently, cells were stained with fluorescent-labeled antibodies
470   against CD3 (17A2, eBiosciences, CA, USA), CD4 (GK1.5, BioLegend, CA, USA), CD8a (53-6.7, BD Bioscience,
471   528 CA, USA), CD44 (IM7, BioLegend, CA, USA), CD11a (M17/4, BioLegend, CA, USA), CD62L (MEL-14,
472   BioLegend, CA, USA), CD127 (SB/199, Biolegend, CA, USA) and KLRG1 (2F1, BioLegend, CA, USA) for 30
473   min at 4°C. Dead cells identified by 7-AAD viability staining solution (BioLegend, CA, USA) were excluded
474   from all analyses. The labeled cells were analyzed by flow cytometry (BD LSRFortessaTM Cell Analyzer)
475   and subsequent analyses were done in detail in FlowJo Software v10.
476

Detection of anti-spike antibodies in mouse sera

478   ELISA (Enzyme-linked ImmunoSorbent Assay) was used to detect SARS-CoV-2 Spike specific IgG response
479   in mouse sera after 6, 12, 24 and 64 weeks post-immunization. As control, sera from mock-immunized
480   mice were included. S1-S2 wildtype and S1-S2 B.1.1.529 variant (Omicron) were used as antigens, which
481   were produced in insect-cells as described before (6, 70), in a baculovirus-free system. For antigen coating,
482   100 ng/well S1-S2 in carbonate buffer (50 mM $NAHCO_3$/Na_2CO_3, pH 9.6) was immobilized overnight at 4
483   °C in 96x well-plates (Greiner Bio-One). ELISA plates were blocked with 2% MPBS-T (2% (w/v) skim milk
484   powder, 0.05% Tween20 in PBS) for 1 h at RT and washed with H_2O containing 0.05% Tween20 using EL405
485   S washer (BioTek). Mice sera were diluted 1:100 and titrated to a final dilution of 1:6400 and incubated

486 for 1h at RT. After washing as described above, the serum IgG respone was detected using horseradish
487 peroxidase (HRP) conjugated goat-anti mouse serum (A0186, Sigma) (1:42000 diluted in 2% MPBS-T) and
488 plates washed again after incubation at RT for 1h. Binding was visualized using tetramethylbenzidine
489 (TMB) substrate (19 parts TMB A solution (30 mM Potassium citrate; 1% (w/v) citric acid (pH 4.1)) and 1
490 part TMB B solution (10 mM TMB; 10% (v/v) Acetone; 90% (v/v) Ethanol; 80 mM H_2O_2 (30%))) and
491 developed for 15 min at RT. Reaction was stopped using 0.5 M/1N sulfuric acid and absorbance measured
492 at 450 nm with subtracting reference at 620 nm using ELISA plate reader (Epoc, BioTek). For K18-hACE2
493 mice challenged with D614G for unspecific binding. EC50 was analyzed by a statistical analysis tool in
494 GraphPad Prism 9. For the aged K18-hACE2 mice challenged with the SARS-CoV-2 VoCs the Area under
495 the curve (AUC) was calculated.
496
497 ***Antibody avidity assay***
498 Antibody avidity assay was performed as described by *Welten et. al.* 2016 (27). In brief, 100 ng/well S1-S2
499 were immobilized in carbonate buffer overnight at 4° and plates blocked with 2% MPBS-T for 1h at RT.
500 Plates were washed with H_2O containing 0.05% Tween20 using EL405 S washer (BioTek). Mice sera
501 showing the best IgG response were selected and always three sera pooled and diluted 1:300 in 2% MPBS-
502 T. After incubation at RT for 1h, plates were washed as described above followed by incubation with
503 NaSCN at RT in indicated dilutions. As control, binding without NaSCN was included. After 15 min
504 incubation, plates were washed immediately two times to ensure complete removal of NaSCN. Binding
505 was detected using goat-anti mouse serum (A0168, Sigma) conjugated with HRP (1:42000 dilution in 2%
506 MPBS-T) at RT for 1h and plates washed as described above. Antibody binding was visualized using TMB
507 substrate as described above and reaction stopped after 15 min at RT using 0.5M/1N sulfuric acid.
508 Absorbance was measured as described above and IgG binding normalized to 100% in absence of NaSCN
509 and avidity calculated as binding after treatment with indicated NaSCN dilutions on described antigens.
510
511 ***In vitro live virus neutralization titer (VNT) assay***
512 The serum neutralization assay was performed as described before (17). Briefly, heat-inactivated sera
513 were serially diluted and incubated with 100 PFU/100 µL of SARS-CoV-2 for 1 h at RT. Thereupon, they
514 were transferred to 96-well plates seeded with Vero-E6 cells and inoculated with serum and virus for 1 h.
515 After the inoculum removal, the cells were overlaid with 1.5% methylcellulose and incubated at 37°C and
516 5% CO_2 for 3 days. The cells were fixed with 4% formaldehyde, followed by crystal violet staining and
517 plaque counting. Serum-neutralizing titer that results in a 50% reduction of virus plaques (VNT50) was
518 analyzed by GraphPad Prism 9 nonlinear regression analysis.
519
520 ***Pseudovirus neutralization assay***
521 Pseudovirus neutralization assays were performed as described in the previous publications (17, 71). For
522 neutralization experiments, pseudotyped particles and heat-inactivated serum dilution were mixed at a
523 1:1 ratio and incubated for 60 min at 37°C before being inoculated onto VeroE6 cells grown in 96-well
524 plates. At 24 h post-infection, GFP expression was measured by using Incucyte S3 (Sartorius, Goettingen,
525 Germany).
526
527 ***bulk RNA extraction and sequencing***
528 To perform RNA bulk sequencing, RNA was isolated from lung tissue and blood using Trizol reagent
529 (Invitrogen) at a 1:3 ratio. Briefly, 3x Trizol LS was added to the homogenized organ sample or blood and
530 vortexed thoroughly. After incubation, 1/5 of the volume of chloroform were added. The samples were

531 vortexed again and incubated for 5 min at RT. Subsequently, tubes were centrifuged at 12,000 × g for 15
532 min at 4°C and aqueous phase were transferred into a new tube and RNA was extracted with the RNA
533 Clean and Concentrator kit (ZYMO Research).
534 Bulk RNA sequencing libraries were constructed using the NEBNext Ultra II Directional RNA Library Prep
535 Kit (New England Biolabs) and sequenced on a high throughput NextSeq 500 device. Reads were aligned
536 to the Mus musculus genome (GRCm39 or mm39) using hisat2 (72) and gene expression quantified using
537 the package featureCounts from Rsubread (73). Analysis was done with DESeq2 (74). Differentially
538 expressed genes were defined by an absolute fold change in mRNA abundance greater than 1.5 (log2 fold
539 change of 0.58 - using DESeq2 shrunken log2 fold changes) and an adjusted p-value of less than 0.05
540 (Benjamini-Hochberg corrected). Gene expression deconvolution was performed with the package GEDIT,
541 using the reference matrix provided for blood analysis (75).

543 *Statistics*
544 One-way ANOVA with Kruskal-Wallis correction was performed for multiple-group analysis. Two-tailed
545 Mann-Whitney tests were used to compare the difference between two independent groups. Log-rank
546 (Mantel-cox) tests were performed to compare the survival distributions of groups. Statistical analysis was
547 calculated by GraphPad Prism 9.

549 *Data availability*
550 All SARS-CoV-2 genome sequences are available as mentioned above. The D614 SARS-CoV-2 variant
551 (GISAID database ID: EPI_ISL_463008), SARS-CoV-2 B.1.351 (Beta) FFM-ZAF1/2021 (GenBank ID:
552 MW822592), and SARS-CoV-2 B.1.1.529 (BA.1) FFM-ZAF0396/2021 (EPI_ISL_6959868; GenBank ID:
553 OL800703).

555 **Author Contributions:** Conceptualization, KM, HJ, YK and LCS; methodology, KM, HJ, YK, LGTA, UK, KE,
556 MZC, MH, FB, MR, MHu, MCB, JM, MS, AK; validation, LCS, ML, SP, MHu; formal analysis, KM, HJ, YK, LGTA;
557 investigation, KM, HJ, YK, LGTA; resources, LCS, ML, SP, MHu, MW, SJ and SC; data curation, KM, HJ, YK,
558 LGTA; writing—original draft preparation, KM and YK; writing—review and editing, all authors;
559 supervision, LCS; project administration, LCS; funding acquisition, LCS, SJ and ML

586

587 **References:**
588 1.   Zhu N, Zhang D, Wang W, Li X, Yang B, Song J, et al. A Novel Coronavirus from Patients with
589 Pneumonia in China, 2019. N Engl J Med. 2020;382(8):727-33.
590 2.   WHO. in World Health Organization 2023 [
591 3.   Volz E, Hill V, McCrone JT, Price A, Jorgensen D, O'Toole A, et al. Evaluating the Effects of SARS-
592 CoV-2 Spike Mutation D614G on Transmissibility and Pathogenicity. Cell. 2021;184(1):64-75 e11.
593 4.   Pegu A, O'Connell SE, Schmidt SD, O'Dell S, Talana CA, Lai L, et al. Durability of mRNA-1273
594 vaccine-induced antibodies against SARS-CoV-2 variants. Science. 2021;373(6561):1372-7.
595 5.   Negi SS, Schein CH, Braun W. Regional and temporal coordinated mutation patterns in SARS-
596 CoV-2 spike protein revealed by a clustering and network analysis. Scientific reports. 2022;12(1):1128.
597 6.   Schubert M, Bertoglio F, Steinke S, Heine PA, Ynga-Durand MA, Maass H, et al. Human serum
598 from SARS-CoV-2-vaccinated and COVID-19 patients shows reduced binding to the RBD of SARS-CoV-2
599 Omicron variant. BMC Med. 2022;20(1):102.
600 7.   Levin EG, Lustig Y, Cohen C, Fluss R, Indenbaum V, Amit S, et al. Waning Immune Humoral
601 Response to BNT162b2 Covid-19 Vaccine over 6 Months. N Engl J Med. 2021;385(24):e84.
602 8.   Shrotri M, Navaratnam AMD, Nguyen V, Byrne T, Geismar C, Fragaszy E, et al. Spike-antibody
603 waning after second dose of BNT162b2 or ChAdOx1. Lancet. 2021;398(10298):385-7.
604 9.   Jacobsen H, Sitaras I, Katzmarzyk M, Cobos Jiménez V, Naughton R, Higdon MM, et al.
605 Systematic review and meta-analysis of the factors affecting waning of post-vaccination neutralizing
606 antibody responses against SARS-CoV-2. npj Vaccines. 2023;8(1):159.
607 10.   Garcia-Beltran WF, Lam EC, St Denis K, Nitido AD, Garcia ZH, Hauser BM, et al. Multiple SARS-
608 CoV-2 variants escape neutralization by vaccine-induced humoral immunity. Cell. 2021;184(9):2523.
609 11.   Jacobsen H, Katzmarzyk M, Higdon MM, Jiménez VC, Sitaras I, Bar-Zeev N, et al. Post-vaccination
610 neutralization responses to Omicron sub-variants. Vaccines. 2022;10(10):1757.
611 12.   Jacobsen H, Strengert M, Maaß H, Ynga Durand MA, Katzmarzyk M, Kessel B, et al. Diminished
612 neutralization responses towards SARS-CoV-2 Omicron VoC after mRNA or vector-based COVID-19
613 vaccinations. Scientific reports. 2022;12(1):19858.
614 13.   Meggiolaro A, Sane Schepisi M, Farina S, Castagna C, Mammone A, Siddu A, et al. Effectiveness
615 of vaccination against SARS-CoV-2 Omicron variant infection, symptomatic disease, and hospitalization:
616 a systematic review and meta-analysis. Expert Rev Vaccines. 2022;21(12):1831-41.
617 14.   Kopanska M, Barnas E, Blajda J, Kuduk B, Lagowska A, Banas-Zabczyk A. Effects of SARS-CoV-2
618 Inflammation on Selected Organ Systems of the Human Body. Int J Mol Sci. 2022;23(8).
619 15.   Ding Q, Zhao H. Long-term effects of SARS-CoV-2 infection on human brain and memory. Cell
620 Death Discov. 2023;9(1):196.

621   16.   Halawa S, Pullamsetti SS, Bangham CRM, Stenmark KR, Dorfmuller P, Frid MG, et al. Potential
622   long-term effects of SARS-CoV-2 infection on the pulmonary vasculature: a global perspective. Nat Rev
623   Cardiol. 2022;19(5):314-31.
624   17.   Kim Y, Zheng X, Eschke K, Chaudhry MZ, Bertoglio F, Tomic A, et al. MCMV-based vaccine vectors
625   expressing full-length viral proteins provide long-term humoral immune protection upon a single-shot
626   vaccination. Cell Mol Immunol. 2022;19(2):234-44.
627   18.   Fisher MA, Lloyd ML. A Review of Murine Cytomegalovirus as a Model for Human
628   Cytomegalovirus Disease-Do Mice Lie? Int J Mol Sci. 2020;22(1).
629   19.   Klenerman P, Oxenius A. T cell responses to cytomegalovirus. Nature reviews Immunology.
630   2016;16(6):367-77.
631   20.   Sylwester AW, Mitchell BL, Edgar JB, Taormina C, Pelte C, Ruchti F, et al. Broadly targeted
632   human cytomegalovirus-specific CD4+ and CD8+ T cells dominate the memory compartments of
633   exposed subjects. J Exp Med. 2005;202(5):673-85.
634   21.   Cicin-Sain L, Sylwester AW, Hagen SI, Siess DC, Currier N, Legasse AW, et al. Cytomegalovirus-
635   specific T cell immunity is maintained in immunosenescent rhesus macaques. Journal of immunology.
636   2011;187(4):1722-32.
637   22.   Karrer U, Sierro S, Wagner M, Oxenius A, Hengel H, Koszinowski UH, et al. Memory inflation:
638   continuous accumulation of antiviral CD8+ T cells over time. Journal of immunology (Baltimore, Md :
639   1950). 2003;170(4):2022-9.
640   23.   Holtappels R, Pahl-Seibert MF, Thomas D, Reddehase MJ. Enrichment of immediate-early 1
641   (m123/pp89) peptide-specific CD8 T cells in a pulmonary CD62L(lo) memory-effector cell pool during
642   latent murine cytomegalovirus infection of the lungs. J Virol. 2000;74(24):11495-503.
643   24.   Cicin-Sain L. Cytomegalovirus memory inflation and immune protection. Medical microbiology
644   and immunology. 2019;208(3-4):339-47.
645   25.   Cicin-Sain L, Brune W, Bubic I, Jonjic S, Koszinowski UH. Vaccination of mice with bacteria
646   carrying a cloned herpesvirus genome reconstituted in vivo. J Virol. 2003;77(15):8249-55.
647   26.   Karrer U, Wagner M, Sierro S, Oxenius A, Hengel H, Dumrese T, et al. Expansion of protective
648   CD8+ T-cell responses driven by recombinant cytomegaloviruses. J Virol. 2004;78(5):2255-64.
649   27.   Hansen SG, Marshall EE, Malouli D, Ventura AB, Hughes CM, Ainslie E, et al. A live-attenuated
650   RhCMV/SIV vaccine shows long-term efficacy against heterologous SIV challenge. Sci Transl Med.
651   2019;11(501).
652   28.   Tsuda Y, Caposio P, Parkins CJ, Botto S, Messaoudi I, Cicin-Sain L, et al. A replicating
653   cytomegalovirus-based vaccine encoding a single Ebola virus nucleoprotein CTL epitope confers
654   protection against Ebola virus. PLoS neglected tropical diseases. 2011;5(8):e1275.
655   29.   Slavuljica I, Busche A, Babic M, Mitrovic M, Gasparovic I, Cekinovic D, et al. Recombinant mouse
656   cytomegalovirus expressing a ligand for the NKG2D receptor is attenuated and has improved vaccine
657   properties. J Clin Invest. 2010;120(12):4532-45.
658   30.   Zheng X, Oduro JD, Boehme JD, Borkner L, Ebensen T, Heise U, et al. Mucosal CD8+ T cell
659   responses induced by an MCMV based vaccine vector confer protection against influenza challenge.
660   PLoS pathogens. 2019;15(9):e1008036.
661   31.   Morabito KM, Ruckwardt TR, Redwood AJ, Moin SM, Price DA, Graham BS. Intranasal
662   administration of RSV antigen-expressing MCMV elicits robust tissue-resident effector and effector
663   memory CD8+ T cells in the lung. Mucosal immunology. 2017;10(2):545-54.
664   32.   Welten SPM, Redeker A, Toes REM, Arens R. Viral Persistence Induces Antibody Inflation
665   without Altering Antibody Avidity. J Virol. 2016;90(9):4402-11.
666   33.   Bongard N, Le-Trilling VTK, Malyshkina A, Rückborn M, Wohlgemuth K, Wensing I, et al.
667   Immunization with a murine cytomegalovirus based vector encoding retrovirus envelope confers strong
668   protection from Friend retrovirus challenge infection. PLoS pathogens. 2019;15(9):e1008043.

669   34.   Gu H, Chen Q, Yang G, He L, Fan H, Deng YQ, et al. Adaptation of SARS-CoV-2 in BALB/c mice for
670   testing vaccine efficacy. Science (New York, NY). 2020;369(6511):1603-7.
671   35.   Tian F, Tong B, Sun L, Shi S, Zheng B, Wang Z, et al. N501Y mutation of spike protein in SARS-
672   CoV-2 strengthens its binding to receptor ACE2. Elife. 2021;10.
673   36.   McCray PB, Jr., Pewe L, Wohlford-Lenane C, Hickey M, Manzel L, Shi L, et al. Lethal infection of
674   K18-hACE2 mice infected with severe acute respiratory syndrome coronavirus. J Virol. 2007;81(2):813-
675   21.
676   37.   Lopera TJ, Chvatal-Medina M, Florez-Alvarez L, Zapata-Cardona MI, Taborda NA, Rugeles MT, et
677   al. Humoral Response to BNT162b2 Vaccine Against SARS-CoV-2 Variants Decays After Six Months. Front
678   Immunol. 2022;13:879036.
679   38.   Tartof SY, Slezak JM, Fischer H, Hong V, Ackerson BK, Ranasinghe ON, et al. Effectiveness of
680   mRNA BNT162b2 COVID-19 vaccine up to 6 months in a large integrated health system in the USA: a
681   retrospective cohort study. Lancet. 2021;398(10309):1407-16.
682   39.   Odainic A, Spitzer J, Szlapa JB, Schade S, Kramer TJ, Neuberger J, et al. Comparative Analysis of
683   Antibody Titers against the Spike Protein of SARS-CoV-2 Variants in Infected Patient Cohorts and Diverse
684   Vaccination Regimes. Int J Mol Sci. 2022;23(20).
685   40.   Bonifacio MA, Laterza R, Vinella A, Schirinzi A, Defilippis M, Di Serio F, et al. Correlation between
686   In Vitro Neutralization Assay and Serological Tests for Protective Antibodies Detection. Int J Mol Sci.
687   2022;23(17).
688   41.   Chernyshev M, Sakharkar M, Connor RI, Dugan HL, Sheward DJ, Rappazzo CG, et al. Vaccination
689   of SARS-CoV-2-infected individuals expands a broad range of clonally diverse affinity-matured B cell
690   lineages. Nat Commun. 2023;14(1):2249.
691   42.   Sakharkar M, Rappazzo CG, Wieland-Alter WF, Hsieh CL, Wrapp D, Esterman ES, et al. Prolonged
692   evolution of the human B cell response to SARS-CoV-2 infection. Sci Immunol. 2021;6(56).
693   43.   Muecksch F, Weisblum Y, Barnes CO, Schmidt F, Schaefer-Babajew D, Wang Z, et al. Affinity
694   maturation of SARS-CoV-2 neutralizing antibodies confers potency, breadth, and resilience to viral
695   escape mutations. Immunity. 2021;54(8):1853-68 e7.
696   44.   Winkler ES, Bailey AL, Kafai NM, Nair S, McCune BT, Yu J, et al. SARS-CoV-2 infection of human
697   ACE2-transgenic mice causes severe lung inflammation and impaired function. Nat Immunol.
698   2020;21(11):1327-35.
699   45.   Nouailles G, Adler JM, Pennitz P, Peidli S, Teixeira Alves LG, Baumgardt M, et al. Live-attenuated
700   vaccine sCPD9 elicits superior mucosal and systemic immunity to SARS-CoV-2 variants in hamsters. Nat
701   Microbiol. 2023;8(5):860-74.
702   46.   Widge AT, Rouphael NG, Jackson LA, Anderson EJ, Roberts PC, Makhene M, et al. Durability of
703   Responses after SARS-CoV-2 mRNA-1273 Vaccination. N Engl J Med. 2021;384(1):80-2.
704   47.   Tregoning JS, Brown ES, Cheeseman HM, Flight KE, Higham SL, Lemm NM, et al. Vaccines for
705   COVID-19. Clinical and experimental immunology. 2020;202(2):162-92.
706   48.   Tregoning JS, Flight KE, Higham SL, Wang Z, Pierce BF. Progress of the COVID-19 vaccine effort:
707   viruses, vaccines and variants versus efficacy, effectiveness and escape. Nature reviews Immunology.
708   2021;21(10):626-36.
709   49.   Andrews N, Stowe J, Kirsebom F, Toffa S, Rickeard T, Gallagher E, et al. Covid-19 Vaccine
710   Effectiveness against the Omicron (B.1.1.529) Variant. N Engl J Med. 2022;386(16):1532-46.
711   50.   Hansen SG, Vieville C, Whizin N, Coyne-Johnson L, Siess DC, Drummond DD, et al. Effector
712   memory T cell responses are associated with protection of rhesus monkeys from mucosal simian
713   immunodeficiency virus challenge. Nat Med. 2009;15(3):293-9.
714   51.   Khoury DS, Cromer D, Reynaldi A, Schlub TE, Wheatley AK, Juno JA, et al. Neutralizing antibody
715   levels are highly predictive of immune protection from symptomatic SARS-CoV-2 infection. Nature
716   medicine. 2021;27(7):1205-11.

717   52.   Tscherne A, Schwarz JH, Rohde C, Kupke A, Kalodimou G, Limpinsel L, et al. Immunogenicity and
718   efficacy of the COVID-19 candidate vector vaccine MVA-SARS-2-S in preclinical vaccination. Proc Natl
719   Acad Sci U S A. 2021;118(28).
720   53.   Carazo S, Talbot D, Boulianne N, Brisson M, Gilca R, Deceuninck G, et al. Single-Dose Messenger
721   RNA Vaccine Effectiveness Against Severe Acute Respiratory Syndrome Coronavirus 2 in Healthcare
722   Workers Extending 16 Weeks Postvaccination: A Test-Negative Design From Quebec, Canada. Clin Infect
723   Dis. 2022;75(1):e805-e13.
724   54.   Lau EH, Hui DS, Tsang OT, Chan WH, Kwan MY, Chiu SS, et al. Long-term persistence of SARS-
725   CoV-2 neutralizing antibody responses after infection and estimates of the duration of protection.
726   EClinicalMedicine. 2021;41:101174.
727   55.   Ferdinands JM, Rao S, Dixon BE, Mitchell PK, DeSilva MB, Irving SA, et al. Waning 2-Dose and 3-
728   Dose Effectiveness of mRNA Vaccines Against COVID-19-Associated Emergency Department and Urgent
729   Care Encounters and Hospitalizations Among Adults During Periods of Delta and Omicron Variant
730   Predominance - VISION Network, 10 States, August 2021-January 2022. MMWR Morb Mortal Wkly Rep.
731   2022;71(7):255-63.
732   56.   Marcotte H, Piralla A, Zuo F, Du L, Cassaniti I, Wan H, et al. Immunity to SARS-CoV-2 up to 15
733   months after infection. iScience. 2022;25(2):103743.
734   57.   Sekine T, Perez-Potti A, Rivera-Ballesteros O, Stralin K, Gorin JB, Olsson A, et al. Robust T Cell
735   Immunity in Convalescent Individuals with Asymptomatic or Mild COVID-19. Cell. 2020;183(1):158-68
736   e14.
737   58.   Moss P. The T cell immune response against SARS-CoV-2. Nat Immunol. 2022;23(2):186-93.
738   59.   McMahan K, Yu J, Mercado NB, Loos C, Tostanoski LH, Chandrashekar A, et al. Correlates of
739   protection against SARS-CoV-2 in rhesus macaques. Nature. 2021;590(7847):630-4.
740   60.   Zhou P, Yang XL, Wang XG, Hu B, Zhang L, Zhang W, et al. A pneumonia outbreak associated with
741   a new coronavirus of probable bat origin. Nature. 2020;579(7798):270-3.
742   61.   Shirato K, Kizaki T. SARS-CoV-2 spike protein S1 subunit induces pro-inflammatory responses via
743   toll-like receptor 4 signaling in murine and human macrophages. Heliyon. 2021;7(2):e06187.
744   62.   Olajide OA, Iwuanyanwu VU, Adegbola OD, Al-Hindawi AA. SARS-CoV-2 Spike Glycoprotein S1
745   Induces Neuroinflammation in BV-2 Microglia. Mol Neurobiol. 2022;59(1):445-58.
746   63.   Lei Y, Zhang J, Schiavon CR, He M, Chen L, Shen H, et al. SARS-CoV-2 Spike Protein Impairs
747   Endothelial Function via Downregulation of ACE 2. Circ Res. 2021;128(9):1323-6.
748   64.   Chaudhry MZ, Eschke K, Hoffmann M, Grashoff M, Abassi L, Kim Y, et al. Rapid SARS-CoV-2
749   Adaptation to Available Cellular Proteases. J Virol. 2022;96(5):e0218621.
750   65.   Widera M, Wilhelm A, Hoehl S, Pallas C, Kohmer N, Wolf T, et al. Limited Neutralization of
751   Authentic Severe Acute Respiratory Syndrome Coronavirus 2 Variants Carrying E484K In Vitro. J Infect
752   Dis. 2021;224(7):1109-14.
753   66.   Wilhelm A, Widera M, Grikscheit K, Toptan T, Schenk B, Pallas C, et al. Limited neutralisation of
754   the SARS-CoV-2 Omicron subvariants BA.1 and BA.2 by convalescent and vaccine serum and monoclonal
755   antibodies. EBioMedicine. 2022;82:104158.
756   67.   Jordan S, Krause J, Prager A, Mitrovic M, Jonjic S, Koszinowski UH, et al. Virus progeny of murine
757   cytomegalovirus bacterial artificial chromosome pSM3fr show reduced growth in salivary Glands due to
758   a fixed mutation of MCK-2. J Virol. 2011;85(19):10346-53.
759   68.   Hoffmann M, Kleine-Weber H, Schroeder S, Kruger N, Herrler T, Erichsen S, et al. SARS-CoV-2
760   Cell Entry Depends on ACE2 and TMPRSS2 and Is Blocked by a Clinically Proven Protease Inhibitor. Cell.
761   2020;181(2):271-80 e8.
762   69.   Hoffmann M, Kruger N, Schulz S, Cossmann A, Rocha C, Kempf A, et al. The Omicron variant is
763   highly resistant against antibody-mediated neutralization: Implications for control of the COVID-19
764   pandemic. Cell. 2022;185(3):447-56 e11.

765   70.   Bertoglio F, Fühner V, Ruschig M, Heine PA, Abassi L, Klünemann T, et al. A SARS-CoV-2
766   neutralizing antibody selected from COVID-19 patients binds to the ACE2-RBD interface and is tolerant
767   to most known RBD mutations. Cell reports. 2021;36(4):109433.
768   71.   Hoffmann M, Arora P, Gross R, Seidel A, Hornich BF, Hahn AS, et al. SARS-CoV-2 variants B.1.351
769   and P.1 escape from neutralizing antibodies. Cell. 2021;184(9):2384-93 e12.
770   72.   Kim D, Paggi JM, Park C, Bennett C, Salzberg SL. Graph-based genome alignment and genotyping
771   with HISAT2 and HISAT-genotype. Nat Biotechnol. 2019;37(8):907-15.
772   73.   Liao Y, Smyth GK, Shi W. The R package Rsubread is easier, faster, cheaper and better for
773   alignment and quantification of RNA sequencing reads. Nucleic Acids Research. 2019;47(8):e47-e.
774   74.   Love MI, Huber W, Anders S. Moderated estimation of fold change and dispersion for RNA-seq
775   data with DESeq2. Genome Biology. 2014;15(12):550.
776   75.   Nadel BB, Lopez D, Montoya DJ, Ma F, Waddel H, Khan MM, et al. The Gene Expression
777   Deconvolution Interactive Tool (GEDIT): accurate cell type quantification from gene expression data.
778   GigaScience. 2021;10(2).

779
780